Phenotypic and genetic associations between anhedonia and brain structure in UK Biobank

Supplementary materials

Table of Contents

Supplementary methods

MRI preprocessing

The T1-weighted volumes were pre-processed and analysed with the FMRIB Software Library (FSL) (http://www.fmrib.ox.ac.uk/fsl). Following removal of face area, gradient distortion correction, the brain was non-linearly warped to the MNI152 "nonlinear 6th generation" standard-space T1-weighted volume template, and the brain area of the images was then extracted for segmentation. Firstly, a tissue-type segmentation using FAST (FMRIB's Automated Segmentation Tool) was applied to extract cerebrospinal fluid, grey matter and white matter; then subcortical structures are extracted using FIRST (FMRIB's Integrated Registration and Segmentation Tool) and the volumes of thalamus, putamen, pallidum, hippocampus, caudate, amygdala and accumbens were calculated for further analysis (https://biobank.ctsu.ox.ac.uk/crystal/crystal/docs/brain_mri.pdf).

Furthermore, the T1 images were also processed with FreeSurfer (http://surfer.nmr.mgh.harvard.edu/). The technical details are described in previous publications [1,2]. Briefly, the processing stream includes motion correction and averaging, removal of non-brain tissue, automated Talairach transformation, intensity normalisation, white matter segmentation, cortical surface reconstruction and parcellation. Cortical thickness was computed in FreeSurfer by calculating the closest distance from the gray/white matter boundary and the gray/CSF boundary at each vertex on the tessellated surface. Researchers compared four parcellation protocols implemented in FreeSurfer and recommended using Desikan-Killiany-Tourville (DKT) protocol approach to derive grey matter thickness [3]. Therefore, this study adopted cortical thickness calculated according to the DKT atlas, with each hemisphere being parcellated into 31 regions (Figure S1).

Diffusion-weighted imaging data was initially corrected for eddy currents, head motion and outlier-slices, and then was processed by UK biobank with a probabilistic tractography based method using the BEDPOSTx tool (Bayesian Estimation of Diffusion Parameters Obtained using Sampling Techniques) and PROBTRACKx [4]. Maps for fractional anisotropy (FA) and mean diffusivity (MD) were generated and FA maps were warped to standard space and used to generate the fibres. Twenty-seven tracts were generated by utilizing the standard-space start/stop ROI masks defined by AutoPtx [5], including forceps major, forceps minor and uncinate fasciculus and 12 bilateral tracts in both hemispheres.

Measures of covariates

Genetic principal components 1–10, calculated via principal component analysis, were included as population stratification covariates.

Head positions in the MRI scanner were included as covariates, including lateral (https://biobank.ctsu.ox.ac.uk/showcase/field.cgi?id=25756), transverse (http://biobank.ctsu.ox.ac.uk/crystal/field.cgi?id=25757) and longitudinal (https://biobank.ctsu.ox.ac.uk/showcase/field.cgi?id=25758) co-ordinates of the centre of the brain mask within the scanner. Intracranial volume consists of grey matter, white matter and ventricular cerebral spinal fluid.

The score of childhood traumatic events was calculated via summing five online follow-up questions (https://biobank.ndph.ox.ac.uk/showcase/label.cgi?id=145): (1) "When I was growing up... I felt loved"; (2) "When I was growing up... People in my family hit me so hard that it left me with bruises or marks"; (3) "When I was growing up... I felt that someone in my family hated me"; (4) "When I was growing up... Someone molested me (sexually)"; (5) "When I was growing up... There was someone to take me to the doctor if I needed it". Participants answered to these questions by selecting “Prefer not to answer”, “Never true”, “Rarely true”, “Sometimes true”, “Often” or “Very often true”. The scores for “feeling loved” and “being taken to doctor when needed” are in an opposite direction, so they were reversed when calculating sum scores.

The score of adulthood traumatic events was also calculated via summing five online follow-up questions (http://biobank.ndph.ox.ac.uk/showcase/label.cgi?id=145): (1) "Since I was sixteen... I have been in a confiding relationship "; (2) "Since I was sixteen... A partner or ex-partner deliberately hit me or used violence in any other way "; (3) "Since I was sixteen... A partner or ex-partner repeatedly belittled me to the extent that I felt worthless "; (4) "Since I was sixteen... A partner or ex-partner sexually interfered with me, or forced me to have sex against my wishes "; (5) "Since I was sixteen... There was money to pay the rent or mortgage when I needed it ". Participants answered to these questions by selecting “Prefer not to answer”, “Never true”, “Rarely true”, “Sometimes true”, “Often” or “Very often true”. The scores for “in a confiding relationship” and “Able to pay rent/mortgage” are in an opposite direction, so they were reversed when calculating sum scores.

Considering only a minority of the sample used medication, we chose to examine impact of ever/never use of medication rather than the specific classes of psychotropic medication. In online follow-up assessments, participants who answered “Yes” to "Have you ever had a time in your life when you felt sad, blue, or depressed for two weeks or more in a row?" and "Have you ever had a time in your life lasting two weeks or more when you lost interest in most things like hobbies, work, or activities that usually give you pleasure?" reported substances taken for depression. Participants chose from “Unprescribed medication (more than once)”, “Medication prescribed to you (for at least two weeks)” or “Drugs or alcohol (more than once)” (https://biobank.ndph.ox.ac.uk/showcase/field.cgi?id=20546). We grouped participants according to use of medication. Those used unprescribed or prescribed medication were classified into one group, while the rest and healthy participants were included in another group.

Depressed mood was assessed by a single question, *" Over the past two weeks, how often have you felt down, depressed or hopeless?".* Participants could choose from the following answers: “not at all”; “several days”; “more than half the days”; and “nearly every day”, which were coded as 0, 1, 2 and 3 respectively.

Townsend deprivation index (http://biobank.ndph.ox.ac.uk/showcase/field.cgi?id=189) at recruitment is a score assigned based on census output regarding their postcode. Education qualification (http://biobank.ndph.ox.ac.uk/showcase/field.cgi?id=6138), current tobacco smoking (http://biobank.ndph.ox.ac.uk/showcase/field.cgi?id=1239) and alcohol intake frequency (http://biobank.ndph.ox.ac.uk/showcase/field.cgi?id=1558) at the first imaging visit were collected using touchscreen questions.

The body mass index (BMI; http://biobank.ndph.ox.ac.uk/showcase/field.cgi?id=21001) at the first imaging visit is calculated using a person's height and weight. The formula is BMI = kg/m^2. Ordinal values of BMI were divided into four categories: underweight (BMI<18.5), normal (18.5≤BMI<25), overweight (25≤BMI<30) and obese (BMI>30).

Medication use, education qualification, current tobacco smoking and alcohol intake frequency and BMI were added to models as categorical variables.

Sensitivity analyses

Analyses regarding anhedonia as a dichotomous variable were performed using same models. We coded anhedonia into ‘0’ and ‘1’, with value ‘0’ referring to participants who reported ‘not at all’ (N = 16488), and a value of ‘1’ representing the remainder of participants (who had reported any anhedonia, N = 3104) and re-analysed its relationship with brain measures from main analyses.

The association between anhedonia and brain structure in healthy participants was also analysed using the same models. To achieve a sample without people with mental illness, we excluded those who self-reported having depression, post-natal depression, schizophrenia, mania/bipolar disorder/manic depression, anxiety/panic attacks, post-traumatic stress disorder, anorexia/bulimia/other eating disorder or obsessive-compulsive disorder. In addition, the interaction between anhedonia and mental illness status (17,489 healthy people vs. 2103 reported any of above disorders) was examined with the same models except adding the mental illness status and an interaction term.

The polygenic risk score for major depressive disorder (PRS-MDD) were calculated using LDpred [6] applied to the summary statistics from a GWAS of major depression [7]. This GWAS contained participants from UK Biobank so we used summary statistics that excluded both UK Biobank and 23andme. We adopted the same quality control criterion used in calculation of PRS-anhedonia and also standardized the scores and excluded values beyond three standard deviations from the sample mean.

Mediation analysis

Previous studies on polygenic risk scores for major depressive disorder or schizophrenia have indicated that brain measures may serve as mediators between genetic risk and psychiatric symptoms. For example, Shen et al. [8] found that MD in anterior thalamic radiation mediated the effect of depression-PRS on current depressive symptoms and that current depressive symptoms mediated the effect of depression-PRS on global MD, MD in thalamic radiations and superior longitudinal fasciculus. Alloza et al. [9] also found the cortical thickness of the insula may mediate the relationship between PRS for schizophrenia and auditory hallucinations. By contrast, no study to date has examined mediation candidates of polygenic risk for anhedonia. Therefore, we conducted the mediation analyses in order to explore possible mediation candidates of PRS-anhedonia and to clarify the relationship between anhedonia, PRS-anhedonia and related brain measures.

Because we have not determined the directional or causal relationship of these associations, we tested whether brain structures might act as mediators between PRS-anhedonia and state anhedonia and whether state anhedonia could mediate the effect of PRS-anhedonia on brain structures. The brain measures were restricted to total grey matter volume (GMV) and total white matter volume (WMV), because only the two were significantly associated with both state anhedonia and PRS-anhedonia after controlling for all covariates. Sex, age, age^2, ICV and scanner positions on the x, y and z axes, genotype array and the first ten genetic principal components were added in the model as covariates. Analyses were conducted using the 'sem' command in Stata and the significance of the mediation effect was estimated using the bootstrap approach (with 1000 random samplings).

Supplementary Results

Demographics regarding confounding covariates

There were significantly positive associations between anhedonia and depressed mood (Pearson's r = 0.662, p < 0.001; Spearman's rho = 0.627, p < 0.001), Townsend social deprivation index (Pearson's r = 0.161, p < 0.001; Spearman's rho = 0.073, p < 0.001), childhood traumatic events (Pearson's r = 0.172, p < 0.001; Spearman's rho = 0.140, p < 0.001) and adulthood traumatic events (Pearson's r = 0.078, p < 0.001; Spearman's rho = 0.157, p < 0.001). There was a significant difference in anhedonia between never/ever medication use groups (two sample t test: ever use group = 1.338 ± 0.011, never use group = 1.166 ± 0.004, t = -18.010, p < 0.001; Using Mann-Whitney U Tests: z = -19.318, p < 0.001). In addition, we found significant differences in anhedonia between different groups for BMI (One-way ANOVA: F = 60.28, p < 0.001; Kruskal-Wallis H test: $\chi2$ = 64.25, *p* < 0.001), current tobacco smoking status (F = 53.32, p < 0.001; Kruskal-Wallis H test: $\chi2$ = 38.69, *p* < 0.001), alcohol intake frequency (F = 21.90, p < 0.001; Kruskal-Wallis H test: $\chi2$ = 40.53, *p* < 0.001), and education qualification (F = 18.18, p < 0.001; Kruskal-Wallis H test: $\chi2$ = 34.49, *p* < 0.001). PRS-MDD was also significantly associated with state anhedonia (β = 0.025, $F_{(1,17293)}$ = 44.37, R-squared = 0.003, p < 0.001). Participants with mental illness (1650 with depression and 453 with other mental disorders) reported higher state anhedonia than healthy individuals (healthy group = 1.162 ± 0.003, group with mental illness = 1.467 ± 0.016, t = -26.9, p < 0.001) and the Mann-Whitney U Test observed same difference (z = -26.344, p < 0.001).

Influence of assessment centers on the associations between state anhedonia, PRS-anhedonia and brain structure

As the Table S4 showed, when the assessment center was included as an additional covariate, we found same brain alterations. As for the differences between the two sites, we firstly examined the interaction between anhedonia/PRS-anhedonia and assessment center on brain structures. Results showed no significant interaction between PRS-anhedonia and assessment center, but significant interaction between anhedonia and assessment center on mean diffusivity in the forceps minor, inferior fronto-occipital fasciculus, inferior longitudinal fasciculus and superior longitudinal fasciculus (Table S5). In addition, we further examined the associations between anhedonia/ PRS-anhedonia and brain structures that we observed in the main analyses (including above four white matter tracts) in the two assessment centers respectively. Results were shown in Table S6-S7. Briefly, for the Cheadle imaging center, we observed similar associations as we found in the main analyses. For the Newcastle center, associations were very weak because of the much smaller sample size. Moreover, looking closely at above four white matter tracts, the associations in two assessment centers seemed to be in different directions, but they were not significant in the Newcastle center.

Associations between state anhedonia (as a dichotomous variable) and brain structure

State anhedonia was associated with reduced total GMV ($\beta = -0.033$, $p_{corrected} < 0.001$; Table S8) and increased total WMV ($\beta = 0.020$, $p_{corrected} = 0.002$), smaller volume of the thalamus ($\beta = -0.056$, $p_{corrected} < 0.001$) and nucleus accumbens ($\beta = -0.069$, $p_{corrected} < 0.001$), and with reduced CT in the rostral anterior cingulate cortex ($\beta = -0.043$, $p_{corrected} = 0.012$) and the opercular part of inferior frontal gyrus ($\beta = -0.048$, $p_{uncorrected} = 0.009$). The paracentral gyrus ($\beta = -0.035$, $p_{uncorrected} = 0.047$) and insula ($\beta = -0.034$, $p_{uncorrected} = 0.048$) was nominally significant before FDR correction while precentral cortex ($\beta = -0.024$, $p_{uncorrected} = 0.167$) was not significant.

With regard to white matter integrity, state anhedonia remained significantly associated with reduced FA in the forceps major ($\beta = -0.045$, $p_{corrected} = 0.029$; Table S4), the anterior thalamic radiation ($\beta = -0.043$, $p_{corrected} = 0.025$), inferior longitudinal fasciculus ($\beta = -0.046$, $p_{corrected} = 0.022$) and posterior thalamic radiation ($\beta = -0.074$, $p_{corrected} < 0.001$) and superior longitudinal fasciculus ($\beta = -0.049$, $p_{corrected} = 0.017$). In addition, we found associations with increased MD in the forceps major ($\beta = 0.049$, $p_{corrected} = 0.019$), forceps minor ($\beta = 0.047$, $p_{corrected} = 0.020$), anterior thalamic radiation ($\beta = 0.080$, $p_{corrected} < 0.001$), cingulate gyrus part of cingulum ($\beta = 0.054$, $p_{corrected} = 0.006$), corticospinal tract ($\beta = 0.057$, $p_{corrected} = 0.005$), inferior fronto-occipital fasciculus ($\beta = 0.059$, $p_{corrected} = 0.003$), inferior longitudinal fasciculus ($\beta = 0.053$, $p_{corrected} = 0.008$), posterior thalamic radiation ($\beta = 0.059$, $p_{corrected} = 0.003$), superior longitudinal fasciculus ($\beta = 0.085$, $p_{corrected} < 0.001$), superior thalamic radiation ($\beta = 0.088$, $p_{corrected} < 0.001$), uncinate fasciculus ($\beta = 0.046$, $p_{corrected} = 0.012$) and right uncinate fasciculus ($\beta = 0.063$, $p_{corrected} = 0.003$). Associations with MD in the left acoustic radiation ($\beta = 0.037$, $p_{uncorrected} = 0.068$) and left uncinate fasciculus ($\beta = 0.029$, $p_{uncorrected} = 0.104$) were not significant.

Associations between state anhedonia (linear variable) and brain structure in healthy participants

For total GMV/WMV, subcortical volumes and regional cortical thickness, we found similar results. State anhedonia was associated with reduced total GMV (β = -0.018, $p_{corrected}$ = 0.002; Table S9) and increased total WMV (β = 0.011, $p_{corrected}$ = 0.034), smaller volume of the thalamus (β = -0.041, $p_{corrected}$ < 0.001) and NAcc (β = -0.057, $p_{corrected}$ < 0.001), and with reduced CT in the paracentral gyrus (β = -0.044, $p_{corrected}$ = 0.005), rostral anterior cingulate cortex (β = -0.045, $p_{corrected}$ = 0.002), opercular part of inferior frontal gyrus (pars opercularis; β = -0.040, $p_{corrected}$ = 0.009), insula (β = -0.033, $p_{corrected}$ = 0.033) and precentral cortex (β = -0.032, $p_{corrected}$ = 0.035).

However, for white matter integrity, only FA in the posterior thalamic radiation (β = -0.045, $p_{uncorrected}$ = 0.048; Table S5) and MD in the Superior thalamic radiation remained significant (β = 0.043, $p_{uncorrected}$ = 0.048). In addition, before FDR correction, nominally significant associations were observed with FA in the forceps major (β = -0.036, $p_{uncorrected}$ = 0.038), as well as MD in the corticospinal tract (β = 0.039, $p_{uncorrected}$ = 0.015), superior longitudinal fasciculus (β = 0.037, $p_{uncorrected}$ = 0.023), anterior thalamic radiation (β = 0.034, $p_{uncorrected}$ = 0.024) and posterior thalamic radiation (β = 0.033, $p_{uncorrected}$ = 0.028). It seems that the association between anhedonia and white matter integrity is weaker when participants with mental disorders were excluded, compared with that of healthy participants (Table 2). Therefore, we subsequently examined the interaction of anhedonia and mental illness status (with/without mental illness) on white matter integrity.

We found nominally significant interaction effects on several white matter tracts before FDR correction (Table S10). Figure S2. illustrates the interaction between anhedonia and mental health status on several white matter tracts, including a) FA in the superior longitudinal fasciculus, b) MD in the cingulate gyrus part of cingulum, c) MD in the inferior longitudinal fasciculus, and d) MD in the uncinate fasciculus.

Associations between PRS-MDD and brain structure

No significant interactions of PRS-MDD and hemisphere were observed for any brain structure. Analyses for white matter integrity found PRS-MDD was associated with lower FA in the posterior thalamic radiation ($\beta = -0.019$, $p_{corrected} = 0.036$; Table S13), and higher MD in the forceps minor ($\beta = 0.023$, $p_{corrected} = 0.013$), anterior thalamic radiation ($\beta = 0.018$, $p_{corrected} = 0.036$), cingulate gyrus part of cingulum ($\beta = 0.023$, $p_{corrected} = 0.012$), corticospinal tract ($\beta = 0.021$, $p_{corrected} = 0.023$), inferior fronto-occipital fasciculus ($\beta = 0.022$, $p_{corrected} = 0.012$), inferior longitudinal fasciculus ($\beta = 0.022$, $p_{corrected} = 0.013$), posterior thalamic radiation ($\beta = 0.023$, $p_{corrected} = 0.010$), superior longitudinal fasciculus ($\beta = 0.027$, $p_{corrected} < 0.001$) and superior thalamic radiation ($\beta = 0.024$, $p_{corrected} = 0.010$).

Mediating candidates of PRS-anhedonia

In the models examining the mediation effect of brain measures, we found that total GMV and total WMV significantly mediated the relationship between PRS-anhedonia and state anhedonia. Coefficients for individual paths are provided in Figure S3a. Total GMV and total WMV may mediate 2.7% and 2.2% of the impact of PRS-anhedonia on state anhedonia respectively. In addition, in the models with state anhedonia as mediators, we found state anhedonia may explain 4.9% of the association between PRS-anhedonia and total GMV, and 4.3% of the association between PRS-anhedonia and total WMV. Coefficients for individual paths are provided in Figure S3b.

Although the mediation effect is very small, it supports the potential mediating role of the brain in the relationship between genetic risk and state anhedonia and the possibility of anhedonia as a mediation candidate of genetic risk for anhedonia. This indicates that the relationship between psychosis and brain phenotypes may not be one-way causality and there may be complex interactions between psychosis and the brain. More studies are needed to clarify the associations between psychiatric disorders and the brain. We will also explore the directional or causal relationship between anhedonia and brain measures and identify putative neural mediators in the future.

Supplementary figures

Figure S1. Regions in the “Desikan-Killiany-Tourville” cortical labeling protocol [10].

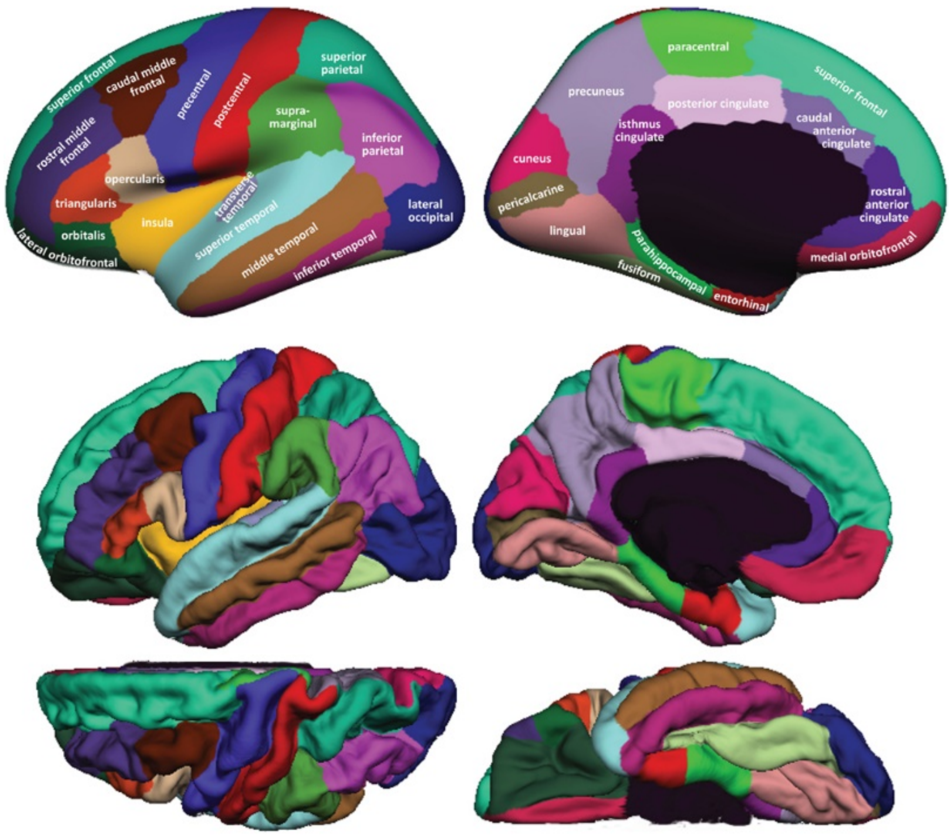

Figure S2. The interaction between anhedonia and mental health status on several white matter tracts, including a) FA in the superior longitudinal fasciculus (SLF), b) MD in the cingulate gyrus part of cingulum (CC), c) MD in the inferior longitudinal fasciculus (ILF), and d) MD in the uncinate fasciculus (UF). These plots suggest that the association between anhedonia and white matter integrity is stronger in participants with mental illness compared with that in those without mental illness. FA, fractional anisotropy; MD, mean diffusivity.

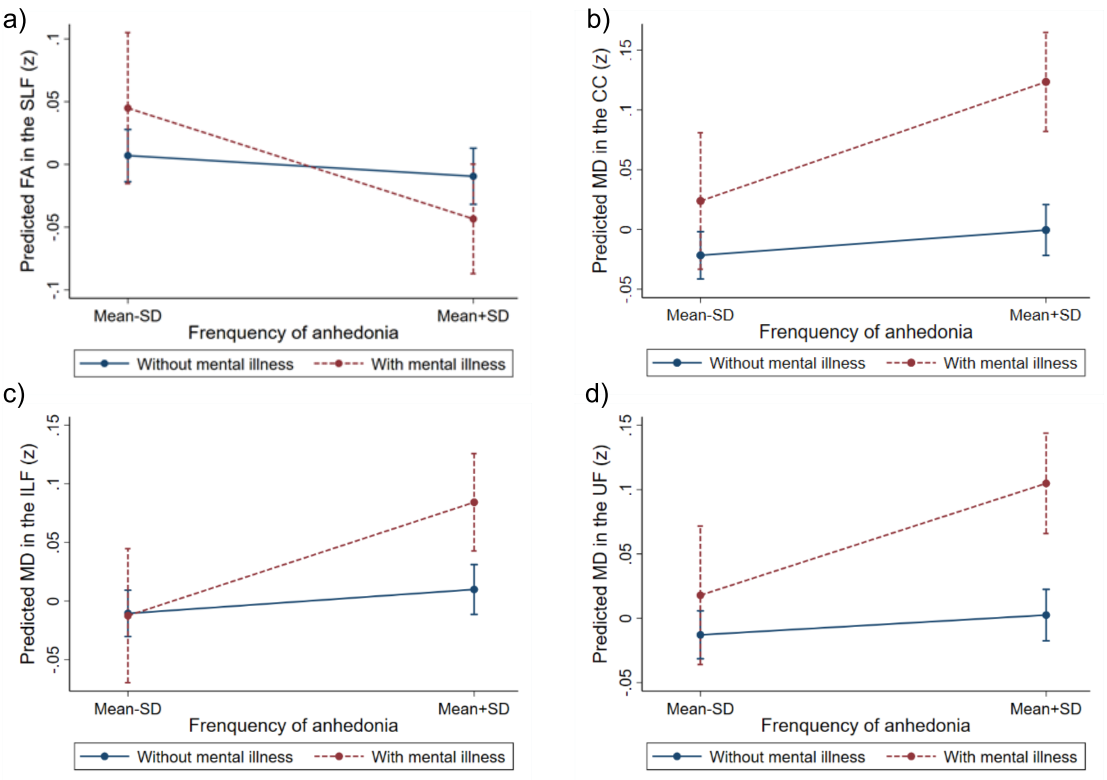

Figure S3. Path diagram of the mediation models of PRS for anhedonia, total grey matter volume, total white matter volume and state anhedonia. a) Total grey/white matter volume partially mediates the effect of PRS for anhedonia on state anhedonia. b) State anhedonia partially mediates the associations between PRS for anhedonia and total grey/white matter. **p < .01. ***p < .001. PRS, polygenic risk score.

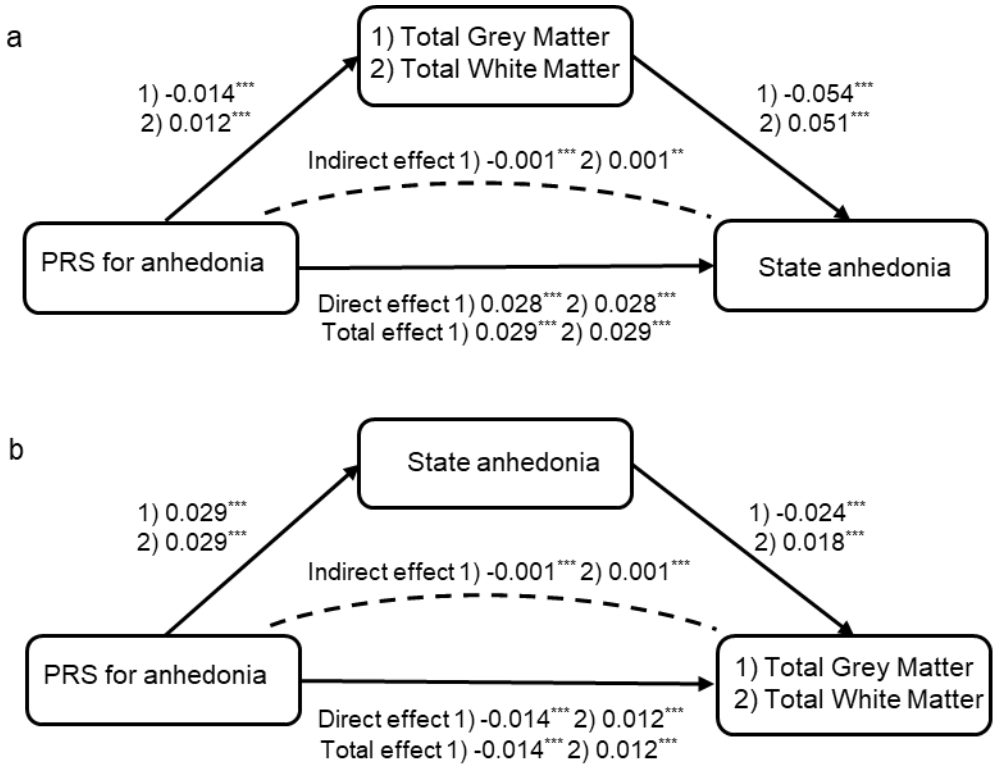

Supplementary tables

Table S1. Participant exclusion criteria according to self-reported cancer and non-cancer illness (data field 20001 and 20002).

Benign neuroma
Brain abscess/intracranial abscess
Brain cancer/primary malignant brain tumour
Brain haemorrhage
Cerebral aneurysm
Cerebral palsy
Chronic/degenerative neurological problem
dementia/alzheimers/cognitive impairment
Encephalitis
Epilepsy
Fracture skull/head
Head injury
Ischaemic stroke
Meningeal cancer/malignant meningioma
Meningioma/benign meningeal tumour
Meningitis
Motor Neurone Disease
Multiple Sclerosis
Nervous system infection
Neurological injury/trauma
Other demyelinating disease (not Multiple Sclerosis)
Other neurological problem
Parkinson's Disease
Spina Bifida
Stroke
Subarachnoid haemorrhage
Subdural haemorrhage/haematoma
Transient ischaemic attack

Table S2. The associations between anhedonia, PRS-anhedonia, brain volumes, cortical thickness and white matter integrity. The models of anhedonia were conducted with age, age^2, sex, total brain volume and head position coordinates set as covariates. The models of PRS-anhedonia also included genotype array and the first ten genetic principal components as covariates. Hemisphere was also set as a covariate when appropriate.

Outcome	State anhedonia						Polygenic risk for anhedonia					
	N	β	SE	Z	p	$p_{corrected}$	N	β	SE	Z	p	$p_{corrected}$
Total grey matter volume	19 564	-0.025	0.005	-5.380	<0.001	<0.001	16 626	-0.014	0.003	-5.520	<0.001	<0.001
Total white matter volume	19 553	0.017	0.004	3.940	<0.001	<0.001	16 613	0.012	0.002	5.320	<0.001	<0.001
Thalamus	19 504	-0.04	0.009	-4.640	<0.001	<0.001	16 574	<0.001	0.005	0.080	0.933	0.968
Caudate	19 469	-0.002	0.011	-0.180	0.861	0.888	16 545	-0.012	0.006	-1.930	0.054	0.157
Putamen	19 481	-0.015	0.01	-1.530	0.126	0.200	16 555	-0.004	0.006	-0.690	0.492	0.694
Pallidum	19 349	-0.016	0.011	-1.390	0.163	0.209	16 441	-0.004	0.006	-0.720	0.470	0.694
Hippocampus	19 375	-0.016	0.011	-1.500	0.135	0.200	16 464	-0.006	0.006	-0.920	0.358	0.551
Amygdala	19 490	-0.019	0.011	-1.740	0.081	0.149	16 564	-0.002	0.006	-0.320	0.749	0.856
Accumbens	19 497	-0.051	0.011	-4.640	<0.001	<0.001	16 568	-0.015	0.006	-2.410	0.016	0.091
Cortical thickness												
Caudal anterior cingulate	19 164	-0.022	0.011	-1.930	0.053	0.128	16 287	<0.001	0.006	-0.070	0.944	0.968
Caudal middle frontal	19 183	-0.018	0.013	-1.410	0.158	0.209	16 294	-0.008	0.007	-1.200	0.231	0.437
Cuneus	19 274	0.018	0.013	1.390	0.166	0.209	16 376	0.005	0.007	0.650	0.513	0.694
Entorhinal	19 112	-0.02	0.012	-1.680	0.093	0.162	16 229	-0.009	0.007	-1.380	0.169	0.356
Fusiform	19 225	-0.019	0.012	-1.530	0.125	0.200	16 333	-0.014	0.007	-2.080	0.037	0.123
Inferior parietal	19 135	-0.015	0.013	-1.140	0.252	0.305	16 250	-0.001	0.007	-0.100	0.919	0.968
Inferior temporal	19 222	-0.027	0.013	-2.180	0.030	0.095	16 331	-0.008	0.007	-1.150	0.251	0.437
Isthmus cingulate	19 245	-0.023	0.012	-1.880	0.060	0.128	16 348	-0.013	0.007	-1.920	0.055	0.157
Lateral occipital	19 258	0.024	0.013	1.900	0.058	0.128	16 363	0.003	0.007	0.460	0.648	0.785
Lateral orbitofrontal	19 258	-0.018	0.013	-1.450	0.147	0.209	16 358	-0.013	0.007	-1.880	0.060	0.160
Lingual	19 275	0.022	0.013	1.740	0.082	0.149	16 374	-0.008	0.007	-1.150	0.251	0.437
Medial orbitofrontal	19 251	-0.023	0.012	-1.870	0.061	0.128	16 356	-0.017	0.007	-2.480	0.013	0.087

Middle temporal	19 272	-0.026	0.012	-2.100	0.036	0.101	16 369	-0.012	0.007	-1.720	0.085	0.213
Parahippocampal	19 265	-0.027	0.012	-2.150	0.031	0.095	16 369	-0.032	0.007	-4.630	<0.001	<0.001
Paracentral	19 243	-0.04	0.013	-3.140	0.002	0.010	16 348	-0.016	0.007	-2.320	0.021	0.093
Pars opercularis	19 160	-0.04	0.012	-3.180	0.001	0.007	16 273	-0.008	0.007	-1.230	0.218	0.436
Pars orbitalis	19 210	-0.018	0.012	-1.500	0.135	0.200	16 320	-0.014	0.007	-2.150	0.032	0.116
Pars triangularis	19 128	-0.017	0.013	-1.380	0.167	0.209	16 242	-0.007	0.007	-1.030	0.304	0.507
Pericalcarine	19 279	0.029	0.013	2.290	0.022	0.080	16 379	<0.001	0.007	0.040	0.969	0.969
Postcentral	19 252	-0.002	0.013	-0.170	0.866	0.888	16 354	-0.004	0.007	-0.620	0.538	0.694
Posterior cingulate	19 266	-0.012	0.012	-0.980	0.327	0.385	16 369	-0.01	0.007	-1.470	0.141	0.313
Precentral	19 185	-0.033	0.013	-2.570	0.010	0.044	16 294	-0.016	0.007	-2.240	0.025	0.100
Precuneus	19 219	-0.011	0.013	-0.870	0.383	0.426	16 323	0.002	0.007	0.320	0.747	0.856
Rostral anterior cingulate	19 232	-0.042	0.012	-3.650	<0.001	<0.001	16 338	-0.006	0.006	-0.940	0.348	0.551
Rostral middle frontal	19 095	-0.01	0.013	-0.770	0.440	0.476	16 221	-0.004	0.007	-0.520	0.602	0.753
Superior frontal	19 183	-0.026	0.013	-2.070	0.038	0.101	16 294	-0.012	0.007	-1.680	0.094	0.221
Superior parietal	19 184	0.012	0.013	0.920	0.357	0.408	16 294	0.005	0.007	0.630	0.531	0.694
Superior temporal	19 248	-0.03	0.012	-2.430	0.015	0.060	16 350	-0.024	0.007	-3.470	0.001	0.008
Supramarginal	19 157	-0.023	0.013	-1.820	0.069	0.138	16 272	-0.001	0.007	-0.110	0.915	0.968
Transverse temporal	19 298	0.001	0.013	0.040	0.968	0.968	16 393	-0.016	0.007	-2.320	0.021	0.093
Insula	19 250	-0.038	0.013	-3.050	0.002	0.010	16 353	-0.03	0.007	-4.340	<0.001	<0.001
Fractional anisotropy												
Forceps major	17 602	-0.043	0.015	-2.890	0.004	0.010	14 945	-0.016	0.008	-1.910	0.057	0.107
Forceps minor	17 680	-0.027	0.014	-1.920	0.055	0.094	15 008	-0.022	0.008	-2.780	0.005	0.021
Middle cerebellar peduncle	17 556	0.012	0.015	0.780	0.434	0.476	14 911	0.005	0.008	0.680	0.498	0.623
Acoustic radiation	17 678	-0.015	0.013	-1.150	0.251	0.341	15 012	0.014	0.007	1.970	0.049	0.098
Anterior thalamic radiation	17 652	-0.039	0.014	-2.820	0.005	0.012	14 986	-0.014	0.008	-1.780	0.076	0.127
Cingulate gyrus part of cingulum	17 716	0.01	0.013	0.820	0.413	0.476	15 041	0.002	0.007	0.270	0.784	0.784
Parahippocampal part of cingulum	17 307	0.018	0.013	1.400	0.162	0.239	14 701	0.009	0.007	1.290	0.196	0.267
Corticospinal tract	17 667	-0.004	0.014	-0.320	0.748	0.771	15 005	-0.003	0.007	-0.470	0.641	0.712

Inferior fronto-occipital fasciculus	17 678	-0.025	0.014	-1.780	0.074	0.120	15 010	-0.014	0.008	-1.800	0.072	0.127
Inferior longitudinal fasciculus	17 656	-0.038	0.014	-2.740	0.006	0.014	14 990	-0.004	0.008	-0.510	0.611	0.705
Medial lemniscus	17 647	-0.013	0.012	-1.060	0.290	0.379	14 992	-0.011	0.007	-1.660	0.096	0.152
Posterior thalamic radiation	17 628	-0.055	0.014	-4.020	<0.001	<0.001	14 968	-0.02	0.008	-2.730	0.006	0.023
Superior longitudinal fasciculus	17 664	-0.036	0.014	-2.540	0.011	0.022	14 998	-0.011	0.008	-1.480	0.139	0.209
Superior thalamic radiation	17 645	-0.009	0.014	-0.610	0.542	0.576	14 987	-0.011	0.008	-1.380	0.167	0.239
Uncinate fasciculus	17 694	-0.012	0.013	-0.970	0.330	0.401	15 021	-0.004	0.007	-0.590	0.557	0.668
Mean diffusivity												
Forceps major	17 567	0.045	0.014	3.150	0.002	0.006	14 916	0.009	0.008	1.150	0.249	0.325
Forceps minor	17 623	0.037	0.014	2.660	0.008	0.017	14 965	0.023	0.008	3.000	0.003	0.021
Middle cerebellar peduncle	17 585	0.025	0.014	1.740	0.082	0.127	14 935	0.025	0.008	3.110	0.002	0.021
Acoustic radiation	17 590	0.013	0.013	1.020	0.308	0.388	14 939	0.014	0.007	1.980	0.048	0.098
Acoustic radiation (left)	17 603	0.035	0.015	2.400	0.016	0.030	—	—	—	—	—	—
Acoustic radiation (right)	17 577	-0.012	0.015	-0.800	0.421	0.476	—	—	—	—	—	—
Anterior thalamic radiation	17 437	0.064	0.013	5.040	<0.001	<0.001	14 937	0.019	0.007	2.700	0.007	0.023
Cingulate gyrus part of cingulum	17 596	0.052	0.013	3.910	<0.001	<0.001	14 939	0.022	0.007	2.990	0.003	0.021
Parahippocampal part of cingulum	17 138	0.015	0.013	1.210	0.224	0.317	14 556	-0.002	0.007	-0.330	0.745	0.784
Corticospinal tract	17 621	0.051	0.014	3.720	<0.001	<0.001	14 966	0.017	0.008	2.210	0.027	0.062
Inferior fronto-occipital fasciculus	17 598	0.049	0.013	3.680	<0.001	<0.001	14 938	0.021	0.007	2.840	0.005	0.021
Inferior longitudinal fasciculus	17 577	0.045	0.013	3.390	0.001	0.003	14 917	0.018	0.007	2.430	0.015	0.038
Medial lemniscus	17 636	-0.002	0.013	-0.180	0.857	0.857	14 977	-0.002	0.007	-0.290	0.775	0.784
Posterior thalamic radiation	17 376	0.046	0.013	3.550	<0.001	<0.001	14 746	0.027	0.007	3.730	<0.001	<0.001
Superior longitudinal fasciculus	17 505	0.064	0.014	4.550	<0.001	<0.001	14 855	0.022	0.008	2.910	0.004	0.021
Superior thalamic radiation	17 440	0.066	0.013	5.270	<0.001	<0.001	14 804	0.018	0.007	2.620	0.009	0.027
Uncinate fasciculus	17 626	0.042	0.012	3.380	0.001	0.003	14 966	0.017	0.007	2.490	0.013	0.035
Uncinate fasciculus (left)	17 632	0.029	0.013	2.240	0.025	0.045	—	—	—	—	—	—
Uncinate fasciculus (right)	17 619	0.056	0.014	4.080	<0.001	<0.001	—	—	—	—	—	—

Table S3. The interaction between anhedonia, PRS-anhedonia and hemisphere on the subcortical volumes, whole-surface cortical thickness and white matter integrity. In all models, age, age^2, sex, total ICV, and lateral, transverse and longitudinal scanner position coordinates were set as covariates. For PRS-anhedonia, genotype array and the first ten genetic principal components were set as covariates additionally. Anhedonia/PRS-anhedonia, hemisphere and the interaction between anhedonia/PRS-anhedonia and hemisphere were also included in the model. As total grey/white matter volume were whole-brain measures, and forceps major, forceps minor and middle cerebellar peduncle were single tracts, these measures were not tested in this model. Significant interaction with anhedonia were found in FA of uncinate fasciculus, MD of acoustic radiation and uncinate fasciculus, therefore individual tests on the value of each hemisphere were conducted for anhedonia and the results were added in Table S3.

Outcome	**State anhedonia**					**Polygenic risk for anhedonia**				
	β	**SE**	**Z**	**p**	**$p_{corrected}$**	**β**	**SE**	**Z**	**p**	**$p_{corrected}$**
Thalamus	-0.002	0.005	-0.310	0.755	0.956	<0.001	0.003	0.050	0.963	0.963
Caudate	-0.007	0.006	-1.100	0.271	0.736	-0.003	0.004	-0.790	0.431	0.953
Putamen	-0.007	0.008	-0.920	0.359	0.778	0.008	0.004	2.030	0.042	0.504
Pallidum	0.013	0.010	1.260	0.208	0.736	-0.005	0.006	-0.860	0.392	0.931
Hippocampus	0.001	0.012	0.090	0.927	0.980	0.015	0.007	2.140	0.032	0.504
Amygdala	0.012	0.016	0.790	0.430	0.778	0.017	0.009	1.940	0.053	0.504
Accumbens	0.006	0.013	0.440	0.660	0.956	-0.003	0.007	-0.440	0.66	0.953
Cortical thickness										
Caudal anterior cingulate	0.006	0.017	0.320	0.746	0.956	0.005	0.009	0.500	0.619	0.953
Caudal middle frontal	-0.013	0.011	-1.140	0.254	0.736	-0.003	0.006	-0.490	0.625	0.953
Cuneus	-0.004	0.013	-0.340	0.735	0.956	-0.007	0.007	-1.030	0.304	0.825
Entorhinal	0.004	0.016	0.260	0.798	0.971	-0.001	0.009	-0.100	0.922	0.963
Fusiform	0.029	0.013	2.190	0.028	0.736	0.01	0.007	1.320	0.187	0.825
Inferior parietal	0.006	0.011	0.520	0.601	0.956	-0.007	0.006	-1.180	0.237	0.825
Inferior temporal	0.018	0.014	1.300	0.192	0.736	-0.002	0.008	-0.270	0.787	0.953
Isthmus cingulate	0.013	0.014	0.880	0.378	0.778	0.002	0.008	0.220	0.825	0.953
Lateral occipital	-0.002	0.012	-0.170	0.865	0.980	-0.001	0.007	-0.210	0.832	0.953

Lateral orbitofrontal	0.018	0.014	1.340	0.179	0.736	-0.008	0.007	-1.030	0.303	0.825
Lingual	-0.001	0.013	-0.090	0.928	0.980	0.003	0.007	0.450	0.651	0.953
Medial orbitofrontal	0.013	0.016	0.810	0.419	0.778	-0.003	0.009	-0.340	0.732	0.953
Middle temporal	0.017	0.014	1.240	0.214	0.736	-0.003	0.008	-0.370	0.712	0.953
Parahippocampal	-0.015	0.014	-1.120	0.264	0.736	0.01	0.008	1.250	0.212	0.825
Paracentral	-0.003	0.011	-0.310	0.753	0.956	-0.007	0.006	-1.160	0.248	0.825
Pars opercularis	0.003	0.013	0.230	0.818	0.971	-0.002	0.007	-0.290	0.775	0.953
Pars orbitalis	0.021	0.015	1.430	0.154	0.736	<0.001	0.008	0.050	0.960	0.963
Pars triangularis	0.002	0.013	0.130	0.893	0.980	-0.002	0.007	-0.330	0.744	0.953
Pericalcarine	-0.004	0.014	-0.320	0.746	0.956	0.001	0.008	0.110	0.911	0.963
Postcentral	<0.001	0.012	0.000	0.997	0.997	-0.006	0.007	-0.920	0.358	0.907
Posterior cingulate	0.012	0.015	0.790	0.429	0.778	-0.017	0.008	-2.010	0.045	0.504
Precentral	0.016	0.011	1.490	0.136	0.736	-0.008	0.006	-1.340	0.180	0.825
Precuneus	0.009	0.010	0.860	0.389	0.778	-0.006	0.005	-1.090	0.275	0.825
Rostral anterior cingulate	-0.008	0.016	-0.520	0.605	0.956	0.004	0.009	0.500	0.620	0.953
Rostral middle frontal	-0.001	0.011	-0.050	0.957	0.983	-0.002	0.006	-0.390	0.698	0.953
Superior frontal	0.011	0.010	1.100	0.270	0.736	-0.006	0.005	-1.130	0.26	0.825
Superior parietal	0.020	0.010	1.950	0.051	0.736	0.004	0.006	0.630	0.529	0.953
Superior temporal	0.023	0.012	1.890	0.059	0.736	-0.004	0.007	-0.640	0.522	0.953
Supramarginal	0.006	0.012	0.520	0.602	0.956	-0.007	0.006	-1.150	0.249	0.825
Transverse temporal	0.012	0.014	0.830	0.406	0.778	-0.001	0.008	-0.190	0.853	0.953
Insula	0.019	0.013	1.420	0.155	0.736	0.002	0.007	0.290	0.769	0.953
Fractional anisotropy										
Acoustic radiation	-0.021	0.014	-1.460	0.143	0.312	0.002	0.008	0.250	0.801	0.987
Anterior thalamic radiation	-0.004	0.009	-0.410	0.681	0.711	-0.002	0.005	-0.450	0.652	0.987
Cingulate gyrus part of cingulum	-0.027	0.014	-1.920	0.055	0.183	<0.001	0.008	0.020	0.985	0.987
Parahippocampal part of cingulum	-0.027	0.015	-1.880	0.061	0.183	0.003	0.008	0.420	0.671	0.987
Corticospinal tract	-0.018	0.010	-1.760	0.078	0.208	0.002	0.006	0.380	0.706	0.987

Inferior fronto-occipital fasciculus	-0.021	0.009	-2.410	0.016	0.077	0.002	0.005	0.390	0.698	0.987
Inferior longitudinal fasciculus	-0.008	0.008	-1.000	0.320	0.515	<0.001	0.005	0.020	0.986	0.987
Medial lemniscus	-0.038	0.015	-2.440	0.015	0.077	-0.018	0.008	-2.110	0.035	0.84
Posterior thalamic radiation	-0.013	0.010	-1.300	0.193	0.356	-0.003	0.006	-0.540	0.588	0.987
Superior longitudinal fasciculus	0.004	0.008	0.540	0.588	0.685	-0.003	0.004	-0.660	0.512	0.987
Superior thalamic radiation	-0.011	0.008	-1.390	0.166	0.332	-0.002	0.004	-0.470	0.639	0.987
Uncinate fasciculus	-0.034	0.013	-2.650	0.008	0.064	-0.005	0.007	-0.770	0.44	0.987
Mean diffusivity										
Acoustic radiation	-0.050	0.015	-3.240	0.001	0.012	0.007	0.009	0.820	0.413	0.987
Anterior thalamic radiation	0.014	0.007	1.970	0.049	0.183	<0.001	0.004	0.100	0.919	0.987
Cingulate gyrus part of cingulum	0.005	0.009	0.510	0.610	0.685	-0.003	0.005	-0.590	0.558	0.987
Parahippocampal part of cingulum	0.011	0.015	0.750	0.453	0.604	-0.006	0.008	-0.690	0.49	0.987
Corticospinal tract	0.010	0.012	0.900	0.367	0.544	-0.001	0.006	-0.150	0.881	0.987
Inferior fronto-occipital fasciculus	0.013	0.008	1.680	0.093	0.223	0.003	0.004	0.620	0.537	0.987
Inferior longitudinal fasciculus	0.003	0.007	0.480	0.628	0.685	<0.001	0.004	0.090	0.927	0.987
Medial lemniscus	0.014	0.015	0.990	0.322	0.515	<0.001	0.008	0.050	0.958	0.987
Posterior thalamic radiation	0.007	0.009	0.690	0.489	0.618	<0.001	0.005	-0.020	0.987	0.987
Superior longitudinal fasciculus	-0.001	0.006	-0.220	0.827	0.827	0.003	0.003	0.900	0.369	0.987
Superior thalamic radiation	0.006	0.007	0.870	0.385	0.544	0.001	0.004	0.130	0.894	0.987
Uncinate fasciculus	0.032	0.010	3.320	0.001	0.012	0.007	0.005	1.290	0.197	0.987

Table S4. The associations between anhedonia, PRS-anhedonia, brain volumes, cortical thickness and white matter integrity. The models of anhedonia were conducted with age, age^2, sex, total brain volume, head position coordinates and assessment center set as covariates. The models of PRS-anhedonia also included genotype array and the first ten genetic principal components as covariates. Hemisphere was also set as a covariate when appropriate.

Outcome	State anhedonia					Polygenic risk for anhedonia				
	β	SE	Z	p	$p_{corrected}$	β	SE	Z	p	$p_{corrected}$
Total grey matter volume	-0.025	0.005	-5.370	<0.001	<0.001	-0.014	0.003	-5.490	<0.001	<0.001
Total white matter volume	0.017	0.004	3.940	<0.001	<0.001	0.012	0.002	5.330	<0.001	<0.001
Thalamus	-0.040	0.009	-4.630	<0.001	<0.001	0.001	0.005	0.140	0.885	0.931
Caudate	-0.002	0.011	-0.190	0.846	0.891	-0.013	0.006	-2.010	0.045	0.153
Putamen	-0.015	0.010	-1.550	0.122	0.203	-0.004	0.006	-0.740	0.459	0.644
Pallidum	-0.016	0.011	-1.400	0.162	0.214	-0.004	0.006	-0.730	0.467	0.644
Hippocampus	-0.017	0.011	-1.510	0.130	0.208	-0.006	0.006	-0.970	0.332	0.553
Amygdala	-0.019	0.011	-1.780	0.075	0.143	-0.003	0.006	-0.460	0.647	0.784
Accumbens	-0.051	0.011	-4.640	<0.001	<0.001	-0.015	0.006	-2.420	0.015	0.100
Cortical thickness										
Caudal anterior cingulate	-0.022	0.011	-1.900	0.058	0.136	<0.001	0.006	0.070	0.944	0.944
Caudal middle frontal	-0.017	0.013	-1.390	0.166	0.214	-0.007	0.007	-1.030	0.303	0.537
Cuneus	0.018	0.013	1.390	0.165	0.214	0.005	0.007	0.690	0.491	0.655
Entorhinal	-0.020	0.012	-1.690	0.091	0.158	-0.010	0.007	-1.440	0.151	0.336
Fusiform	-0.019	0.012	-1.500	0.135	0.208	-0.013	0.007	-1.920	0.055	0.169
Inferior parietal	-0.014	0.013	-1.110	0.267	0.324	0.001	0.007	0.120	0.908	0.931
Inferior temporal	-0.027	0.012	-2.140	0.032	0.098	-0.007	0.007	-1.020	0.309	0.537
Isthmus cingulate	-0.023	0.012	-1.870	0.061	0.136	-0.012	0.007	-1.860	0.063	0.180
Lateral occipital	0.024	0.013	1.890	0.059	0.136	0.003	0.007	0.420	0.677	0.796
Lateral orbitofrontal	-0.018	0.013	-1.420	0.156	0.214	-0.012	0.007	-1.710	0.087	0.232
Lingual	0.022	0.013	1.740	0.081	0.147	-0.008	0.007	-1.140	0.256	0.512
Medial orbitofrontal	-0.022	0.012	-1.840	0.066	0.139	-0.015	0.007	-2.310	0.021	0.116

Middle temporal	-0.025	0.012	-2.050	0.040	0.107	-0.01	0.007	-1.520	0.128	0.306
Parahippocampal	-0.026	0.012	-2.140	0.032	0.098	-0.031	0.007	-4.600	<0.001	<0.001
Paracentral	-0.040	0.013	-3.130	0.002	0.011	-0.016	0.007	-2.240	0.025	0.116
Pars opercularis	-0.039	0.012	-3.150	0.002	0.011	-0.007	0.007	-1.020	0.308	0.537
Pars orbitalis	-0.018	0.012	-1.470	0.142	0.210	-0.013	0.007	-2.000	0.046	0.153
Pars triangularis	-0.017	0.013	-1.350	0.177	0.221	-0.006	0.007	-0.850	0.394	0.623
Pericalcarine	0.029	0.013	2.320	0.020	0.073	0.001	0.007	0.150	0.881	0.931
Postcentral	-0.002	0.013	-0.150	0.884	0.907	-0.004	0.007	-0.500	0.614	0.768
Posterior cingulate	-0.011	0.012	-0.950	0.341	0.390	-0.009	0.007	-1.350	0.178	0.375
Precentral	-0.033	0.013	-2.560	0.010	0.044	-0.015	0.007	-2.160	0.031	0.124
Precuneus	-0.011	0.013	-0.840	0.403	0.448	0.004	0.007	0.520	0.605	0.768
Rostral anterior cingulate	-0.042	0.012	-3.630	<0.001	<0.001	-0.005	0.006	-0.830	0.405	0.623
Rostral middle frontal	-0.010	0.013	-0.750	0.455	0.492	-0.003	0.007	-0.370	0.714	0.816
Superior frontal	-0.026	0.013	-2.050	0.040	0.107	-0.011	0.007	-1.510	0.130	0.306
Superior parietal	0.012	0.013	0.960	0.339	0.390	0.006	0.007	0.800	0.426	0.631
Superior temporal	-0.030	0.012	-2.400	0.016	0.064	-0.023	0.007	-3.300	0.001	0.008
Supramarginal	-0.023	0.013	-1.780	0.075	0.143	0.001	0.007	0.120	0.903	0.931
Transverse temporal	0.001	0.013	0.060	0.951	0.951	-0.015	0.007	-2.220	0.026	0.116
Insula	-0.038	0.013	-3.020	0.003	0.015	-0.029	0.007	-4.200	<0.001	<0.001
Fractional anisotropy										
Forceps major	-0.044	0.015	-2.970	0.003	0.008	-0.017	0.008	-2.140	0.032	0.074
Forceps minor	-0.028	0.014	-1.930	0.054	0.092	-0.022	0.008	-2.840	0.005	0.021
Middle cerebellar peduncle	0.011	0.015	0.730	0.464	0.509	0.004	0.008	0.530	0.594	0.636
Acoustic radiation	-0.016	0.013	-1.260	0.209	0.296	0.012	0.007	1.650	0.098	0.163
Anterior thalamic radiation	-0.039	0.014	-2.850	0.004	0.010	-0.015	0.008	-1.910	0.056	0.105
Cingulate gyrus part of cingulum	0.010	0.013	0.790	0.427	0.496	0.001	0.007	0.190	0.846	0.846
Parahippocampal part of cingulum	0.018	0.013	1.390	0.164	0.242	0.009	0.007	1.230	0.220	0.287
Corticospinal tract	-0.006	0.013	-0.440	0.656	0.656	-0.006	0.007	-0.850	0.394	0.455

Inferior fronto-occipital fasciculus	-0.025	0.014	-1.800	0.072	0.117	-0.014	0.008	-1.840	0.065	0.115
Inferior longitudinal fasciculus	-0.039	0.014	-2.760	0.006	0.014	-0.005	0.008	-0.600	0.551	0.612
Medial lemniscus	-0.011	0.012	-0.920	0.358	0.435	-0.009	0.007	-1.260	0.206	0.281
Posterior thalamic radiation	-0.054	0.014	-3.970	<0.001	<0.001	-0.019	0.008	-2.510	0.012	0.036
Superior longitudinal fasciculus	-0.036	0.014	-2.550	0.011	0.022	-0.012	0.008	-1.520	0.129	0.204
Superior thalamic radiation	-0.009	0.014	-0.630	0.530	0.563	-0.012	0.008	-1.470	0.142	0.213
Uncinate fasciculus	-0.014	0.013	-1.080	0.281	0.367	-0.006	0.007	-0.910	0.363	0.436
Mean diffusivity										
Forceps major	0.046	0.014	3.230	0.001	0.003	0.011	0.008	1.350	0.176	0.251
Forceps minor	0.036	0.014	2.610	0.009	0.019	0.022	0.008	2.880	0.004	0.021
Middle cerebellar peduncle	0.024	0.014	1.670	0.095	0.147	0.023	0.008	2.860	0.004	0.021
Acoustic radiation	0.013	0.013	1.040	0.298	0.375	0.014	0.007	2.040	0.042	0.084
Acoustic radiation (left)	0.036	0.015	2.410	0.016	0.030	—	—	—	—	—
Acoustic radiation (right)	-0.011	0.015	-0.780	0.438	0.496	—	—	—	—	—
Anterior thalamic radiation	0.064	0.013	5.070	<0.001	<0.001	0.020	0.007	2.800	0.005	0.021
Cingulate gyrus part of cingulum	0.052	0.013	3.880	<0.001	<0.001	0.022	0.007	2.940	0.003	0.021
Parahippocampal part of cingulum	0.015	0.013	1.220	0.224	0.305	-0.002	0.007	-0.300	0.768	0.794
Corticospinal tract	0.050	0.014	3.690	<0.001	<0.001	0.016	0.008	2.100	0.036	0.077
Inferior fronto-occipital fasciculus	0.049	0.013	3.640	<0.001	<0.001	0.020	0.007	2.720	0.007	0.026
Inferior longitudinal fasciculus	0.045	0.013	3.360	0.001	0.003	0.017	0.007	2.320	0.020	0.050
Medial lemniscus	-0.006	0.012	-0.480	0.629	0.648	-0.008	0.007	-1.110	0.266	0.333
Posterior thalamic radiation	0.044	0.013	3.430	0.001	0.003	0.023	0.007	3.230	0.001	0.021
Superior longitudinal fasciculus	0.062	0.014	4.480	<0.001	<0.001	0.020	0.008	2.650	0.008	0.027
Superior thalamic radiation	0.065	0.013	5.210	<0.001	<0.001	0.016	0.007	2.370	0.018	0.049
Uncinate fasciculus	0.043	0.012	3.490	<0.001	<0.001	0.019	0.007	2.820	0.005	0.021
Uncinate fasciculus (left)	0.030	0.013	2.310	0.021	0.038	—	—	—	—	—
Uncinate fasciculus (right)	0.058	0.014	4.220	<0.001	<0.001	—	—	—	—	—

Table S5. The interaction between anhedonia, PRS-anhedonia, and the assessment center on brain volumes, cortical thickness and white matter integrity. The models of anhedonia were conducted with age, age2, sex, total brain volume and head position coordinates set as covariates. The models of PRS-anhedonia also included genotype array and the first ten genetic principal components as covariates. Hemisphere was also set as a covariate when appropriate.

Outcome	State anhedonia					Polygenic risk for anhedonia				
	β	SE	Z	p	$p_{corrected}$	β	SE	Z	p	$p_{corrected}$
Total grey matter volume	0.014	0.012	1.130	0.260	0.954	-0.003	0.007	-0.370	0.710	0.978
Total white matter volume	-0.006	0.011	-0.570	0.571	0.954	0.003	0.006	0.460	0.645	0.978
Thalamus	0.021	0.023	0.910	0.365	0.954	0.006	0.013	0.470	0.641	0.978
Caudate	0.047	0.030	1.580	0.115	0.954	0.003	0.017	0.150	0.884	0.978
Putamen	0.026	0.026	0.990	0.320	0.954	0.005	0.015	0.330	0.738	0.978
Pallidum	0.018	0.029	0.630	0.530	0.954	-0.020	0.017	-1.150	0.250	0.978
Hippocampus	0.037	0.029	1.260	0.208	0.954	0.004	0.017	0.260	0.794	0.978
Amygdala	-0.025	0.029	-0.850	0.394	0.954	-0.025	0.017	-1.480	0.140	0.978
Accumbens	0.009	0.029	0.330	0.743	0.954	-0.011	0.017	-0.660	0.512	0.978
Cortical thickness										
Caudal anterior cingulate	-0.005	0.030	-0.170	0.864	0.974	-0.026	0.017	-1.520	0.129	0.978
Caudal middle frontal	<0.001	0.033	<0.001	0.998	0.998	-0.029	0.019	-1.510	0.130	0.978
Cuneus	-0.007	0.034	-0.210	0.836	0.974	0.013	0.020	0.680	0.499	0.978
Entorhinal	0.010	0.032	0.310	0.754	0.954	-0.017	0.019	-0.920	0.356	0.978
Fusiform	-0.018	0.033	-0.560	0.575	0.954	0.003	0.019	0.180	0.859	0.978
Inferior parietal	0.002	0.033	0.050	0.960	0.985	-0.011	0.020	-0.550	0.583	0.978
Inferior temporal	-0.034	0.033	-1.040	0.299	0.954	-0.015	0.019	-0.780	0.434	0.978
Isthmus cingulate	0.018	0.032	0.550	0.583	0.954	0.011	0.019	0.580	0.560	0.978
Lateral occipital	0.009	0.034	0.270	0.787	0.954	-0.008	0.020	-0.390	0.698	0.978
Lateral orbitofrontal	0.027	0.033	0.820	0.411	0.954	0.006	0.019	0.300	0.764	0.978
Lingual	-0.028	0.033	-0.860	0.390	0.954	-0.005	0.019	-0.270	0.791	0.978

Medial orbitofrontal	-0.023	0.032	-0.720	0.469	0.954	0.001	0.019	0.060	0.954	0.978
Middle temporal	-0.040	0.032	-1.250	0.212	0.954	0.001	0.019	0.080	0.939	0.978
Parahippocampal	0.004	0.032	0.110	0.913	0.974	-0.036	0.019	-1.890	0.058	0.978
Paracentral	0.005	0.034	0.140	0.885	0.974	-0.007	0.020	-0.340	0.732	0.978
Pars opercularis	0.057	0.033	1.750	0.079	0.954	-0.012	0.019	-0.630	0.531	0.978
Pars orbitalis	0.035	0.032	1.110	0.268	0.954	-0.002	0.019	-0.120	0.908	0.978
Pars triangularis	0.009	0.033	0.290	0.773	0.954	0.014	0.019	0.710	0.480	0.978
Pericalcarine	0.015	0.033	0.450	0.651	0.954	0.023	0.019	1.170	0.241	0.978
Postcentral	0.014	0.033	0.420	0.675	0.954	0.004	0.019	0.210	0.834	0.978
Posterior cingulate	-0.014	0.031	-0.460	0.647	0.954	0.013	0.018	0.730	0.464	0.978
Precentral	0.036	0.034	1.070	0.287	0.954	-0.002	0.020	-0.130	0.899	0.978
Precuneus	0.011	0.034	0.340	0.736	0.954	0.004	0.020	0.220	0.828	0.978
Rostral anterior cingulate	0.014	0.031	0.470	0.636	0.954	-0.029	0.018	-1.620	0.106	0.978
Rostral middle frontal	0.022	0.034	0.640	0.521	0.954	-0.003	0.020	-0.140	0.887	0.978
Superior frontal	0.011	0.033	0.320	0.746	0.954	-0.012	0.019	-0.640	0.520	0.978
Superior parietal	0.003	0.034	0.090	0.925	0.974	-0.001	0.020	-0.070	0.948	0.978
Superior temporal	0.009	0.033	0.270	0.785	0.954	-0.006	0.019	-0.310	0.753	0.978
Supramarginal	0.041	0.033	1.240	0.217	0.954	0.007	0.019	0.380	0.703	0.978
Transverse temporal	0.041	0.033	1.250	0.210	0.954	0.000	0.019	<0.001	0.998	0.998
Insula	0.033	0.033	0.980	0.326	0.954	-0.003	0.019	-0.170	0.867	0.978
Fractional anisotropy										
Forceps major	0.077	0.038	2.030	0.042	0.095	-0.031	0.022	-1.400	0.163	0.623
Forceps minor	0.077	0.037	2.090	0.036	0.094	-0.022	0.021	-1.030	0.301	0.758
Middle cerebellar peduncle	0.056	0.038	1.470	0.141	0.228	-0.038	0.022	-1.720	0.085	0.623
Acoustic radiation	-0.003	0.032	-0.100	0.923	0.951	-0.040	0.019	-2.080	0.037	0.555
Anterior thalamic radiation	0.042	0.035	1.200	0.230	0.326	-0.023	0.021	-1.130	0.257	0.758
Cingulate gyrus part of cingulum	0.032	0.033	0.980	0.325	0.409	-0.022	0.019	-1.140	0.254	0.758
Parahippocampal part of cingulum	0.011	0.032	0.330	0.744	0.816	-0.007	0.019	-0.380	0.705	0.824

Corticospinal tract	0.014	0.034	0.420	0.676	0.766	-0.030	0.020	-1.480	0.140	0.623
Inferior fronto-occipital fasciculus	0.095	0.036	2.660	0.008	0.054	-0.030	0.021	-1.440	0.150	0.623
Inferior longitudinal fasciculus	0.086	0.036	2.410	0.016	0.064	-0.032	0.021	-1.510	0.130	0.623
Medial lemniscus	-0.007	0.032	-0.210	0.831	0.883	-0.019	0.018	-1.030	0.303	0.758
Posterior thalamic radiation	0.057	0.035	1.640	0.100	0.189	-0.049	0.020	-2.420	0.016	0.480
Superior longitudinal fasciculus	0.086	0.036	2.380	0.017	0.064	-0.012	0.021	-0.560	0.576	0.824
Superior thalamic radiation	0.033	0.036	0.910	0.365	0.443	-0.029	0.021	-1.380	0.166	0.623
Uncinate fasciculus	0.069	0.033	2.110	0.035	0.094	-0.017	0.019	-0.910	0.364	0.758
Mean diffusivity										
Forceps major	-0.063	0.037	-1.720	0.086	0.172	0.009	0.022	0.430	0.670	0.824
Forceps minor	-0.103	0.036	-2.900	0.004	0.043	0.008	0.021	0.370	0.714	0.824
Middle cerebellar peduncle	-0.001	0.037	-0.040	0.970	0.970	-0.020	0.022	-0.920	0.357	0.758
Acoustic radiation	-0.033	0.032	-1.010	0.311	0.407	0.002	0.019	0.130	0.896	0.896
Acoustic radiation (left)	-0.018	0.038	-0.470	0.640	0.750	—	—	—	—	—
Acoustic radiation (right)	-0.050	0.038	-1.330	0.185	0.286	—	—	—	—	—
Anterior thalamic radiation	-0.082	0.033	-2.510	0.012	0.063	-0.006	0.019	-0.320	0.747	0.830
Cingulate gyrus part of cingulum	-0.052	0.034	-1.520	0.128	0.218	0.003	0.020	0.140	0.891	0.896
Parahippocampal part of cingulum	-0.037	0.032	-1.150	0.250	0.340	0.010	0.019	0.550	0.583	0.824
Corticospinal tract	-0.042	0.035	-1.220	0.224	0.326	0.005	0.020	0.240	0.807	0.865
Inferior fronto-occipital fasciculus	-0.109	0.034	-3.150	0.002	0.034	0.008	0.020	0.400	0.690	0.824
Inferior longitudinal fasciculus	-0.096	0.034	-2.810	0.005	0.043	0.008	0.020	0.410	0.680	0.824
Medial lemniscus	-0.068	0.032	-2.140	0.032	0.094	0.016	0.019	0.880	0.379	0.758
Posterior thalamic radiation	-0.081	0.033	-2.470	0.013	0.063	0.015	0.019	0.790	0.429	0.804
Superior longitudinal fasciculus	-0.108	0.036	-3.030	0.002	0.034	0.013	0.021	0.600	0.548	0.824
Superior thalamic radiation	-0.072	0.032	-2.250	0.025	0.085	0.008	0.019	0.450	0.655	0.824
Uncinate fasciculus	-0.061	0.032	-1.910	0.057	0.121	0.009	0.019	0.470	0.639	0.824
Uncinate fasciculus (left)	-0.053	0.033	-1.620	0.106	0.190	—	—	—	—	—
Uncinate fasciculus (right)	-0.072	0.035	-2.060	0.040	0.095	—	—	—	—	—

Table S6. The associations between anhedonia and brain structures in the Cheadle and Newcastle imaging centers. The model was conducted with age, age^2, sex, total brain volume and head position coordinates set as covariates. Hemisphere was also set as a covariate when appropriate.

Outcome	Cheadle				Newcastle			
	β	SE	Z	p	β	SE	Z	p
Total grey matter volume	-0.028	0.005	-5.32	<0.001	-0.015	0.011	-1.33	0.185
Total white matter volume	0.018	0.005	3.77	<0.001	0.013	0.010	1.34	0.180
Thalamus	-0.044	0.010	-4.60	<0.001	-0.022	0.020	-1.05	0.294
Accumbens	-0.053	0.012	-4.43	<0.001	-0.033	0.026	-1.26	0.207
Cortical thickness								
Paracentral	-0.041	0.014	-2.92	0.004	-0.037	0.031	-1.18	0.237
Pars opercularis	-0.048	0.014	-3.50	<0.001	0.004	0.028	0.14	0.887
Precentral	-0.038	0.014	-2.72	0.006	-0.009	0.031	-0.29	0.775
Rostral anterior cingulate	-0.046	0.013	-3.59	<0.001	-0.021	0.027	-0.77	0.443
Insula	-0.044	0.014	-3.17	0.002	-0.009	0.030	-0.30	0.764
Fractional anisotropy								
Forceps major	-0.059	0.016	-3.61	<0.001	0.022	0.035	0.62	0.537
Anterior thalamic radiation	-0.047	0.015	-3.13	0.002	>-0.001	0.033	-0.01	0.995
Inferior longitudinal fasciculus	-0.054	0.015	-3.54	<0.001	0.030	0.033	0.90	0.367
Posterior thalamic radiation	-0.064	0.015	-4.30	<0.001	-0.011	0.033	-0.34	0.731
Superior longitudinal fasciculus	-0.050	0.015	-3.27	0.001	0.028	0.033	0.86	0.392
Mean diffusivity								
Forceps major	0.059	0.016	3.73	<0.001	-0.008	0.034	-0.23	0.815
Forceps minor	0.054	0.015	3.49	<0.001	-0.036	0.031	-1.17	0.240
Acoustic radiation (left)	0.040	0.017	2.40	0.016	0.017	0.031	0.54	0.592
Anterior thalamic radiation	0.080	0.014	5.64	<0.001	-0.002	0.029	-0.06	0.951
Cingulate gyrus part of cingulum	0.061	0.015	4.11	<0.001	0.014	0.030	0.48	0.631
Corticospinal tract	0.059	0.015	3.89	<0.001	0.014	0.031	0.45	0.651

Inferior fronto-occipital fasciculus	0.069	0.015	4.62	<0.001	-0.035	0.031	-1.12	0.265
Inferior longitudinal fasciculus	0.058	0.014	4.12	<0.001	-0.011	0.030	-0.36	0.718
Posterior thalamic radiation	0.082	0.015	5.32	<0.001	-0.021	0.032	-0.64	0.524
Superior longitudinal fasciculus	0.079	0.014	5.66	<0.001	0.012	0.029	0.41	0.683
Superior thalamic radiation	0.056	0.014	4.02	<0.001	-0.010	0.029	-0.36	0.720
Uncinate fasciculus	0.040	0.014	2.84	0.004	-0.018	0.030	-0.62	0.534
Uncinate fasciculus (left)	0.072	0.015	4.71	<0.001	-0.005	0.031	-0.17	0.864
Uncinate fasciculus (right)	-0.028	0.005	-5.32	<0.001	-0.015	0.011	-1.33	0.185

Table S7. The associations between PRS-anhedonia and brain structures in the Cheadle and Newcastle imaging centers. The model was conducted with age, age^2, sex, total brain volume, head position coordinates, genotype array, the first ten genetic principal components and assessment center set as covariates. Hemisphere was also set as a covariate when appropriate.

Outcome	Cheadle				Newcastle			
	β	SE	Z	p	β	SE	Z	p
Total grey matter volume	-0.014	0.003	-4.93	<0.001	-0.017	0.007	-2.44	0.015
Total white matter volume	0.012	0.003	4.75	<0.001	0.015	0.006	2.48	0.013
Cortical thickness								
Parahippocampal	-0.026	0.007	-3.52	<0.001	-0.061	0.017	-3.56	<0.001
Superior temporal	-0.023	0.007	-3.17	0.002	-0.031	0.017	-1.86	0.063
Insula	-0.029	0.007	-3.83	<0.001	-0.034	0.018	-1.95	0.051
Fractional anisotropy								
Forceps minor	-0.019	0.009	-2.26	0.024	-0.038	0.020	-1.94	0.053
Posterior thalamic radiation	-0.010	0.008	-1.28	0.199	-0.061	0.019	-3.14	0.002
Mean diffusivity								
Forceps minor	0.021	0.008	2.51	0.012	0.026	0.018	1.45	0.148
Middle cerebellar peduncle	0.026	0.009	3.00	0.003	0.008	0.021	0.38	0.705
Anterior thalamic radiation	0.021	0.008	2.73	0.006	0.015	0.017	0.87	0.385
Cingulate gyrus part of cingulum	0.019	0.008	2.34	0.019	0.022	0.017	1.27	0.202
Inferior fronto-occipital fasciculus	0.018	0.008	2.25	0.024	0.027	0.018	1.45	0.146
Inferior longitudinal fasciculus	0.015	0.008	1.93	0.053	0.025	0.018	1.36	0.175
Posterior thalamic radiation	0.022	0.008	2.84	0.004	0.038	0.018	2.16	0.031
Superior longitudinal fasciculus	0.017	0.008	2.08	0.038	0.031	0.019	1.62	0.105
Superior thalamic radiation	0.015	0.008	2.01	0.045	0.025	0.017	1.45	0.148
Uncinate fasciculus	0.018	0.007	2.42	0.015	0.026	0.017	1.54	0.123

Table S8. The association between anhedonia as a dichotomous variable and significant regions from the main analysis of anhedonia. The same model was conducted with age, age^2, sex, total ICV and head position coordinates set as covariates. Hemisphere was also set as a covariate when appropriate.

Outcome	β	SE	Z	P	$p_{corrected}$
grey matter	-0.033	0.006	-5.140	<0.001	<0.001
white matter	0.020	0.006	3.430	0.001	0.002
Thalamus	-0.056	0.012	-4.690	<0.001	<0.001
Accumbens	-0.069	0.015	-4.600	<0.001	<0.001
Paracentral	-0.035	0.018	-1.990	0.047	0.054
Pars opercularis	-0.048	0.017	-2.820	0.005	0.009
Precentral	-0.024	0.018	-1.380	0.167	0.167
Rostral anterior cingulate	-0.043	0.016	-2.660	0.008	0.012
Insula	-0.034	0.017	-1.970	0.048	0.054
Forceps major	-0.045	0.020	-2.250	0.025	0.028
Anterior thalamic radiation	-0.043	0.019	-2.300	0.021	0.025
Inferior longitudinal fasciculus	-0.046	0.019	-2.400	0.017	0.022
Posterior thalamic radiation	-0.074	0.019	-3.960	<0.001	<0.001
Superior longitudinal fasciculus	-0.049	0.019	-2.560	0.011	0.017
Forceps major	0.049	0.020	2.490	0.013	0.019
Forceps minor	0.047	0.019	2.440	0.015	0.020
Acoustic radiation (left)	0.037	0.020	1.830	0.068	0.072
Anterior thalamic radiation	0.080	0.017	4.580	<0.001	<0.001
Cingulate gyrus part of cingulum	0.054	0.018	2.990	0.003	0.006
Corticospinal tract	0.057	0.019	3.030	0.002	0.005
Inferior fronto-occipital fasciculus	0.059	0.018	3.200	0.001	0.003
Inferior longitudinal fasciculus	0.053	0.018	2.910	0.004	0.008
Posterior thalamic radiation	0.059	0.018	3.320	0.001	0.003
Superior longitudinal fasciculus	0.085	0.019	4.470	<0.001	<0.001
Superior thalamic radiation	0.088	0.017	5.100	<0.001	<0.001
Uncinate fasciculus	0.046	0.017	2.680	0.007	0.012
Uncinate fasciculus (left)	0.029	0.018	1.620	0.104	0.104
Uncinate fasciculus (right)	0.063	0.019	3.360	0.001	0.003

Table S9. The association between anhedonia and significant regions emerged from the main analysis of anhedonia in healthy individuals. The same model was conducted with age, age^2, sex, total ICV and head position coordinates set as covariates. Hemisphere was also set as a covariate when appropriate.

Outcome	N	β	SE	Z-value	p	$p_{corrected}$
grey matter	17 464	-0.018	0.006	-3.220	0.001	0.002
white matter	17 452	0.011	0.005	2.170	0.030	0.034
Thalamus	17 437	-0.041	0.010	-4.000	<0.001	<0.001
Accumbens	17 473	-0.057	0.013	-4.470	<0.001	<0.001
Paracentral	17 249	-0.044	0.015	-2.920	0.003	0.005
Pars opercularis	17 200	-0.040	0.015	-2.760	0.006	0.009
Precentral	17 224	-0.032	0.015	-2.110	0.035	0.035
Rostral anterior cingulate	17 260	-0.045	0.014	-3.290	0.001	0.002
Insula	17 250	-0.033	0.015	-2.230	0.026	0.033
Forceps major	15 698	-0.036	0.017	-2.070	0.038	0.103
Anterior thalamic radiation	15 793	-0.018	0.016	-1.130	0.260	0.309
Inferior longitudinal fasciculus	15 801	-0.022	0.016	-1.330	0.185	0.284
Posterior thalamic radiation	15 802	-0.045	0.016	-2.830	0.005	0.048
Superior longitudinal fasciculus	15 800	-0.016	0.016	-1.000	0.317	0.335
Forceps major	15 675	0.030	0.017	1.790	0.073	0.173
Forceps minor	15 725	0.019	0.016	1.170	0.242	0.308
Acoustic radiation (left)	15 703	0.020	0.017	1.170	0.243	0.308
Anterior thalamic radiation	15 659	0.034	0.015	2.250	0.024	0.089
Cingulate gyrus part of cingulum	15 759	0.021	0.016	1.330	0.183	0.284
Corticospinal tract	15 798	0.039	0.016	2.440	0.015	0.089
Inferior fronto-occipital fasciculus	15 766	0.024	0.016	1.510	0.132	0.251
Inferior longitudinal fasciculus	15 749	0.020	0.016	1.300	0.194	0.284
Posterior thalamic radiation	15 687	0.033	0.015	2.200	0.028	0.089
Superior longitudinal fasciculus	15 699	0.037	0.016	2.270	0.023	0.089
Superior thalamic radiation	15 639	0.043	0.015	2.910	0.004	0.048
Uncinate fasciculus	15 807	0.015	0.015	1.010	0.311	0.335
Uncinate fasciculus (left)	15 729	0.002	0.015	0.150	0.878	0.878
Uncinate fasciculus (right)	15 714	0.026	0.016	1.640	0.100	0.211

Table S10. The interaction between anhedonia and mental health status on significant measures from the main analysis for anhedonia. Age, age^2, sex, total ICV and lateral, transverse and longitudinal scanner position coordinates were set as covariates. Anhedonia, mental health status and the interaction between anhedonia and mental health status were also included in the model. Hemisphere was also set as a covariate when appropriate.

Outcome	β	SE	Z-value	p	$p_{corrected}$
grey matter	-0.025	0.011	-2.260	0.024	0.108
white matter	0.025	0.010	2.530	0.012	0.108
Thalamus	0.009	0.021	0.430	0.666	0.856
Accumbens	0.032	0.026	1.240	0.214	0.642
Paracentral	0.008	0.030	0.270	0.784	0.882
Pars opercularis	0.003	0.029	0.120	0.908	0.908
Precentral	-0.016	0.030	-0.530	0.599	0.856
Rostral anterior cingulate	0.016	0.027	0.590	0.557	0.856
Insula	-0.017	0.030	-0.580	0.561	0.856
Forceps major	0.005	0.035	0.140	0.890	0.890
Anterior thalamic radiation	-0.042	0.032	-1.310	0.192	0.304
Inferior longitudinal fasciculus	-0.046	0.033	-1.390	0.164	0.283
Posterior thalamic radiation	-0.015	0.032	-0.460	0.642	0.681
Superior longitudinal fasciculus	-0.072	0.033	-2.180	0.029	0.069
Forceps major	0.035	0.034	1.030	0.305	0.446
Forceps minor	0.032	0.033	0.980	0.329	0.447
Acoustic radiation (left)	0.029	0.035	0.840	0.401	0.508
Anterior thalamic radiation	0.061	0.030	2.050	0.041	0.087
Cingulate gyrus part of cingulum	0.078	0.031	2.510	0.012	0.065
Corticospinal tract	0.015	0.032	0.460	0.645	0.681
Inferior fronto-occipital fasciculus	0.070	0.032	2.220	0.026	0.069
Inferior longitudinal fasciculus	0.076	0.031	2.440	0.015	0.065
Posterior thalamic radiation	0.022	0.030	0.710	0.478	0.568
Superior longitudinal fasciculus	0.078	0.033	2.400	0.017	0.065
Superior thalamic radiation	0.058	0.029	1.970	0.049	0.093
Uncinate fasciculus	0.071	0.029	2.430	0.015	0.065
Uncinate fasciculus (left)	0.067	0.030	2.210	0.027	0.069
Uncinate fasciculus (right)	0.080	0.032	2.490	0.013	0.065

Table S11. The association between anhedonia and significant regions emerged from the main analysis of anhedonia, with age, age[2], sex, total brain volume head position coordinates, anhedonia, depressed mood, childhood traumatic events, adulthood traumatic events, medication use, body mass index, current tobacco use, alcohol intake frequency, education qualification and Townsend deprivation index considered as covariates. Hemisphere was also set as a covariate when appropriate.

Outcome	N	β	SE	Z-value	p	$p_{corrected}$
grey matter	12,472	-0.025	0.008	-3.070	0.002	0.009
white matter	12,466	0.018	0.007	2.520	0.012	0.022
Thalamus	12,458	-0.015	0.015	-0.970	0.333	0.333
Accumbens	12,479	-0.043	0.019	-2.240	0.025	0.038
Paracentral	12,322	-0.062	0.022	-2.810	0.005	0.011
Pars opercularis	12,291	-0.070	0.022	-3.220	0.001	0.009
Precentral	12,309	-0.063	0.022	-2.830	0.005	0.011
Rostral anterior cingulate	12,329	-0.029	0.020	-1.430	0.153	0.172
Insula	12,327	-0.041	0.022	-1.870	0.061	0.078
Forceps major	11,250	-0.001	0.026	-0.040	0.970	0.994
Anterior thalamic radiation	11,310	-0.015	0.024	-0.610	0.544	0.820
Inferior longitudinal fasciculus	11,327	-0.012	0.024	-0.480	0.629	0.820
Posterior thalamic radiation	11,322	0.000	0.024	-0.010	0.994	0.994
Superior longitudinal fasciculus	11,317	-0.028	0.024	-1.150	0.251	0.667
Forceps major	11,218	0.034	0.025	1.340	0.180	0.667
Forceps minor	11,274	0.017	0.024	0.710	0.478	0.820
Acoustic radiation (left)	11,239	0.014	0.026	0.530	0.596	0.820
Anterior thalamic radiation	11,230	0.024	0.022	1.080	0.281	0.667
Cingulate gyrus part of cingulum	11,298	0.016	0.023	0.690	0.488	0.820
Corticospinal tract	11,311	0.006	0.024	0.270	0.786	0.895
Inferior fronto-occipital fasciculus	11,299	0.006	0.023	0.250	0.801	0.895
Inferior longitudinal fasciculus	11,282	0.014	0.023	0.600	0.546	0.820
Posterior thalamic radiation	11,256	0.010	0.022	0.460	0.647	0.820
Superior longitudinal fasciculus	11,259	0.028	0.024	1.170	0.243	0.667
Superior thalamic radiation	11,213	0.039	0.022	1.810	0.071	0.519
Uncinate fasciculus	11,320	0.038	0.022	1.740	0.082	0.519
Uncinate fasciculus (left)	11,272	0.033	0.023	1.460	0.146	0.667
Uncinate fasciculus (right)	11,257	0.047	0.024	1.980	0.048	0.519

Table S12. The associations between PRS-anhedonia and brain structure controlling for extra confounding factors. The models were conducted with age, age^2, sex, total brain volume head position coordinates, anhedonia, depressed mood, childhood traumatic events, adulthood traumatic events, medication use, body mass index, current tobacco use, alcohol intake frequency, education qualification and Townsend deprivation index, genotype array and the first ten genetic principal components as covariates. Hemisphere was also set as a covariate when appropriate.

Outcome	N	β	SE	Z-value	p	$p_{corrected}$
grey matter	10 640	-0.007	0.003	-2.330	0.020	0.020
white matter	10 633	0.009	0.003	3.000	0.003	0.005
Parahippocampal	10 512	-0.031	0.009	-3.540	<0.001	<0.001
Superior temporal	10 503	-0.023	0.009	-2.630	0.009	0.011
Insula	10 510	-0.027	0.009	-3.080	0.002	0.005
Forceps minor	9 644	-0.020	0.010	-1.980	0.048	0.057
Posterior thalamic radiation	9 661	-0.009	0.009	-0.980	0.326	0.326
Forceps minor	9 620	0.019	0.010	1.950	0.052	0.057
Middle cerebellar peduncle	9 576	0.024	0.010	2.430	0.015	0.057
Anterior thalamic radiation	9 577	0.020	0.009	2.250	0.025	0.057
Cingulate gyrus part of cingulum	9 638	0.026	0.009	2.780	0.005	0.057
Inferior fronto-occipital fasciculus	9 638	0.021	0.009	2.210	0.027	0.057
Inferior longitudinal fasciculus	9 620	0.018	0.009	2.010	0.044	0.057
Posterior thalamic radiation	9 598	0.019	0.009	2.190	0.029	0.057
Superior longitudinal fasciculus	9 601	0.021	0.010	2.160	0.030	0.057
Superior thalamic radiation	9 563	0.018	0.009	2.120	0.034	0.057
Uncinate fasciculus	9 655	0.018	0.009	2.020	0.044	0.057

Table S13. The associations between PRS-MDD and subcortical volumes, whole-surface cortical thickness and white matter integrity. The models of anhedonia were conducted with age, age^2, sex, total brain volume, head position coordinates, genotype array and the first ten genetic principal components set as covariates. Hemisphere was also set as a covariate when appropriate.

Outcome	N	β	SE	Z	p	$p_{corrected}$
grey matter	16617	-0.002	0.003	-0.920	0.356	0.843
white matter	16604	0.002	0.002	0.760	0.445	0.843
Thalamus	16566	-0.007	0.005	-1.440	0.149	0.662
Caudate	16536	0.007	0.006	1.090	0.277	0.843
Putamen	16548	0.007	0.006	1.260	0.206	0.687
Pallidum	16433	-0.009	0.006	-1.510	0.132	0.662
Hippocampus	16454	<0.001	0.006	0.020	0.983	0.983
Amygdala	16555	-0.006	0.006	-0.970	0.332	0.843
Accumbens	16558	-0.001	0.006	-0.100	0.919	0.967
Cortical thickness						
Caudal anterior cingulate	16276	-0.003	0.006	-0.530	0.598	0.886
Caudal middle frontal	16284	0.004	0.007	0.600	0.548	0.843
Cuneus	16366	0.009	0.007	1.300	0.194	0.687
Entorhinal	16218	0.005	0.007	0.700	0.482	0.843
Fusiform	16323	0.002	0.007	0.260	0.798	0.960
Inferior parietal	16241	0.013	0.007	1.840	0.065	0.608
Inferior temporal	16321	-0.003	0.007	-0.390	0.695	0.956
Isthmus cingulate	16338	-0.004	0.007	-0.610	0.545	0.843
Lateral occipital	16353	0.017	0.007	2.370	0.018	0.360
Lateral orbitofrontal	16348	-0.005	0.007	-0.760	0.445	0.843
Lingual	16364	0.012	0.007	1.770	0.076	0.608
Medial orbitofrontal	16346	-0.005	0.007	-0.760	0.450	0.843
Middle temporal	16360	0.002	0.007	0.350	0.730	0.956
Parahippocampal	16359	-0.002	0.007	-0.290	0.770	0.960
Paracentral	16339	0.002	0.007	0.330	0.741	0.956
Pars opercularis	16263	<0.001	0.007	-0.060	0.953	0.977
Pars orbitalis	16310	-0.006	0.007	-0.920	0.359	0.843
Pars triangularis	16232	-0.001	0.007	-0.150	0.878	0.967
Pericalcarine	16369	0.010	0.007	1.470	0.142	0.662
Postcentral	16345	0.010	0.007	1.480	0.139	0.662
Posterior cingulate	16358	-0.016	0.007	-2.480	0.013	0.360
Precentral	16284	0.002	0.007	0.230	0.816	0.960
Precuneus	16313	0.007	0.007	0.920	0.356	0.843
Rostral anterior cingulate	16328	-0.004	0.006	-0.640	0.521	0.843
Rostral middle frontal	16211	0.001	0.007	0.120	0.902	0.967
Superior frontal	16284	0.001	0.007	0.110	0.914	0.967
Superior parietal	16284	0.010	0.007	1.390	0.166	0.664
Superior temporal	16340	-0.006	0.007	-0.840	0.399	0.843
Supramarginal	16261	0.005	0.007	0.670	0.501	0.843

Transverse temporal	16383	0.003	0.007	0.490	0.624	0.891
Insula	16343	-0.015	0.007	-2.100	0.036	0.480
Fractional anisotropy						
Forceps major	14938	-0.001	0.008	-0.150	0.883	0.913
Forceps minor	15001	-0.016	0.008	-2.050	0.040	0.092
Middle cerebellar peduncle	14901	-0.003	0.008	-0.310	0.755	0.809
Acoustic radiation	15004	0.006	0.007	0.880	0.380	0.493
Anterior thalamic radiation	14980	-0.008	0.008	-1.110	0.267	0.381
Cingulate gyrus part of cingulum	15033	-0.008	0.007	-1.180	0.239	0.377
Parahippocampal part of cingulum	14694	0.004	0.007	0.550	0.584	0.649
Corticospinal tract	14998	-0.008	0.007	-1.010	0.311	0.424
Inferior fronto-occipital fasciculus	15003	-0.010	0.008	-1.300	0.194	0.342
Inferior longitudinal fasciculus	14983	-0.012	0.008	-1.580	0.115	0.230
Medial lemniscus	14983	-0.005	0.007	-0.800	0.427	0.493
Posterior thalamic radiation	14962	-0.019	0.008	-2.540	0.011	0.036
Superior longitudinal fasciculus	14990	-0.009	0.008	-1.220	0.224	0.373
Superior thalamic radiation	14979	-0.014	0.008	-1.810	0.071	0.152
Uncinate fasciculus	15013	<0.001	0.007	-0.010	0.989	0.989
Mean diffusivity						
Forceps major	14909	0.006	0.008	0.800	0.424	0.493
Forceps minor	14958	0.023	0.008	2.960	0.003	0.013
Middle cerebellar peduncle	14929	0.009	0.008	1.110	0.265	0.381
Acoustic radiation	14931	0.010	0.007	1.430	0.151	0.283
Anterior thalamic radiation	14795	0.018	0.007	2.520	0.012	0.036
Cingulate gyrus part of cingulum	14931	0.023	0.007	3.080	0.002	0.012
Parahippocampal part of cingulum	14549	-0.015	0.007	-2.090	0.036	0.090
Corticospinal tract	14959	0.021	0.008	2.770	0.006	0.023
Inferior fronto-occipital fasciculus	14930	0.022	0.007	3.030	0.002	0.012
Inferior longitudinal fasciculus	14909	0.022	0.007	3.000	0.003	0.013
Medial lemniscus	14970	0.006	0.007	0.810	0.415	0.493
Posterior thalamic radiation	14740	0.023	0.007	3.270	0.001	0.010
Superior longitudinal fasciculus	14848	0.027	0.008	3.540	<0.001	<0.001
Superior thalamic radiation	14796	0.024	0.007	3.420	0.001	0.010
Uncinate fasciculus	14959	0.016	0.007	2.260	0.024	0.065

Supplementary References

1. Fischl, B. et al. Whole brain segmentation: automated labeling of neuroanatomical structures in the human brain. *Neuron* **33**, 341-355 (2002).

2. Fischl, B. FreeSurfer. *Neuroimage* **62**, 774-781 (2012).

3. Mikhael, S. S. & Pernet, C. A controlled comparison of thickness, volume and surface areas from multiple cortical parcellation packages. *BMC Bioinformatics* **20**, 55 (2019).

4. Jbabdi, S., Sotiropoulos, S. N., Savio, A. M., Graña, M. & Behrens, T. E. Model ‐ based analysis of multishell diffusion MR data for tractography: how to get over fitting problems. *Magn. Reson. Med.* **68**, 1846-1855 (2012).

5. de Groot, M. et al. Improving alignment in tract-based spatial statistics: evaluation and optimization of image registration. *Neuroimage* **76**, 400-411 (2013).

6. Vilhjálmsson, B. J. et al. Modeling linkage disequilibrium increases accuracy of polygenic risk scores. *Am. J. Hum. Genet.* **97**, 576-592 (2015).

7. Wray, N. R. et al. Genome-wide association analyses identify 44 risk variants and refine the genetic architecture of major depression. *Nature genetics* **50**, 668-681 (2018).

8. Shen, X. et al. A phenome-wide association and Mendelian Randomisation study of polygenic risk for depression in UK Biobank. *Nat. Commun.* **11**, 2301 (2020).

9. Alloza, C. et al. Psychotic-like experiences, polygenic risk scores for schizophrenia, and structural properties of the salience, default mode, and central-executive networks in healthy participants from UK Biobank. *Transl. Psychiatry* **10**, 1-13 (2020).

10. Klein, A. & Tourville, J. 101 labeled brain images and a consistent human cortical labeling protocol. *Front. Neurosci.* **6**, 171 (2012).